REGULAR ARTICLE

blood advances

Mechano-covalent protection of coagulation factor VIII by von Willebrand factor

Diego Butera,[1] Haoqing Jerry Wang,[2-4] Heng-Giap Woon,[1] Yunduo Charles Zhao,[2,3] Lining Arnold Ju,[2-5] and Philip J. Hogg[1]

[1]The Centenary Institute, Camperdown, NSW, Australia; [2]Charles Perkins Centre and [3]School of Biomedical Engineering, Faculty of Engineering, University of Sydney, Sydney, NSW, Australia; [4]Heart Research Institute, Newtown, NSW, Australia; and [5]The University of Sydney Nano Institute (Sydney Nano), University of Sydney, Sydney, NSW, Australia

Key Points

- Bleeding arrest is critically dependent on FVIII binding to VWF in the shear forces of the circulation.
- FVIII binding involves dynamic changes in the covalent states of several VWF disulfides that is required for a productive interaction.

von Willebrand factor (VWF) is the protective carrier of procoagulant factor VIII (FVIII) in the shear forces of the circulation, prolonging its half-life and delivering it to the developing thrombus. Using force spectroscopy, VWF-FVIII complex formation is characterized by catch-bond behavior in which force first decelerates then accelerates bond dissociation. Patients with mutations in VWF at the FVIII binding site phenocopies hemophilia A and the most common mutations are of cysteine residues involving multiple disulfide bonds. From differential cysteine alkylation and mass spectrometry experiments, 13 VWF disulfide bonds at the FVIII binding site were found to exist in formed and unformed states, and binding of FVIII results in partial formation of 12 of the VWF bonds. Force spectroscopy studies indicate that the VWF-FVIII bond stiffens in response to force and this feature of the interaction is ablated when VWF disulfide bonds are prevented from forming, resulting in slip-only bond behavior. Exposure of VWF to pathological fluid shear forces ex vivo and in vivo causes partial cleavage of all 13 disulfide bonds, further supporting their malleable nature. These findings demonstrate that FVIII binding to VWF involves dynamic changes in the covalent states of several VWF disulfides that are required for productive interaction in physiological shear forces.

Introduction

von Willebrand factor (VWF) is a circulating plasma glycoprotein produced by vascular endothelial cells and megakaryocytes that chaperones blood coagulation cofactor factor VIII (FVIII) and tethers platelets to the damaged vessel wall.[2] It circulates as a series of multimers containing variable numbers of 500 kDa dimeric units. Any size multimer is able to chaperone FVIII,[3] while only the largest multimers effectively tether platelets in the shear forces of flowing blood due to their polyvalency.

The importance of chaperoning FVIII is illustrated by patients with von Willebrand disease (VWD), the most common inherited bleeding disorder in humans, which results from defective and/or deficient VWF protein.[2] Patients with severe VWD are deficient in VWF and FVIII and intravenously administered FVIII has considerably shortened survival in the vasculature (from 12-14 hours to <3 hours). Patients with type 2N VWD with mutations that impair FVIII binding phenocopies hemophilia A, a genetic

Submitted 26 July 2022; accepted 10 September 2022; prepublished online on *Blood Advances* First Edition 14 October 2022; final version published online 11 May 2023. https://doi.org/10.1182/bloodadvances.2022008650.

The mass spectrometry proteomics data have been deposited to the Proteome Xchange Consortium via the PRIDE[1] partner repository with the data set identifier PXD034866.

Data are available on request from the corresponding author, Philip Hogg (phil.hogg@sydney.edu.au).

The full-text version of this article contains a data supplement.

deficiency in FVIII.[4] Understanding the nature of VWF-FVIII complex formation is essential for linking genetic and clinical phenotypes and designing new approaches to treat VWD.

The FVIII binding region on VWF was identified within a tryptic fragment comprising residues 767 to 1031.[5] This fragment encompasses the TIL' and E' domains that have been shown to be essential for FVIII binding in functional[6,7] and structural[8] studies. The most severe VWD type 2N phenotypes that have the lowest circulating plasma FVIII levels are due to mutations in TIL'[4] and TIL' is the epitope for potent FVIII binding-blocking monoclonal antibodies.[9,10] VWF binding site mutations frequently involve disulfide bond cysteines, with 18 cysteine mutants involving 14 disulfide bonds in the TIL' through E3 domains (residues 764-1252) reported. Disulfide bonds are the covalent links between the sulfur atoms of pairs of cysteine amino acids. All the disulfide bonds in the TIL'-TIL3 domains of VWF are intact in solution and crystal structures of the recombinant proteins.[7,11] Largely based on this information, it has been assumed that the VWD cysteine mutations ablate the disulfide bond that the residue participates in and alters the structure of the binding site which impairs affinity for FVIII.

By investigating FVIII binding to VWF under shear forces experienced by the proteins in the circulation we have revealed key aspects of the interaction that help to explain the striking dependence on VWF disulfide bonds for productive binding. VWF-FVIII complex formation is characterized by a catch bond in which force first decelerates then accelerates bond dissociation and this behavior is dependent on dynamic covalent changes in VWF disulfide bonds.

Methods

Recombinant and plasma VWF proteins

Full-length human VWF DNA was cloned into pcDNA3.1 vector according to manufacturer's specifications and the construct purified using PureLink Quick Plasmid Miniprep Kit (Machery-Nagel). For transfection into HEK293, cells were grown at 37°C with 5% CO_2 in Dulbecco's modified Eagle's medium supplemented with 10% fetal bovine serum (GE Healthcare) and penicillin-streptomycin antibiotics (Gibco). Cells at 60% confluence were transfected using polyethylenimine at a ratio of 12.5 mg DNA:50 mg polyethylenimine (Polysciences) in OptiMEM media (Thermofisher). The transfected HEK293 cells were washed with phosphate-buffered saline and incubated for 72 hours in serum-free Opti-MEM. The conditioned media was collected (20 mL) and concentrated 10-fold using Snakeskin tubing (Thermofisher) overlayed with polyethylene glycol 20 000 (Sigma) at 4°C. This material was dialyzed overnight at 4°C in 20 mM Tris, 50 mM NaCl, pH 7.8 buffer and further concentrated using Ultracel spin filters with 100-kDa cut-off membrane (Millipore). Aliquots were stored at −80°C.

Biostate (500 IU, CSL-Behring) was resuspended in 10 mL of Milli-Q water. The sample was applied to a 600 mL Sepharose CL-2B column pre-equilibrated in 20 mM Hepes pH 7.4 buffer containing 140 mM NaCl and 0.02% NaN_3. The eluate was monitored by absorbance at 280 nm, flow rate was 0.5 mL/min and 4 mL fractions were collected. The VWF in the leading edge of the eluted protein peak was collected and concentrated ~10-fold using Snakeskin tubing (Thermofisher) overlayed with polyethylene glycol 20 000 (Sigma) at 4°C. VWF protein purity (>95%) was confirmed by reducing SDS-PAGE and aliquots were stored at −80°C. Purified VWF (0.3 mL of 1.2 mg/mL in 50 mM Hepes, pH 7.4 buffer containing 0.14 M NaCl and 10 mM $CaCl_2$) was incubated with 5 mM ^{12}C-IPA for 1 hour at 22°C in the dark to alkylate unpaired Cys thiols in the protein. The unreacted IPA was removed using a 7 kDa MWCO Zeba spin desalting column (Thermofisher). Protein concentration was measured by absorbance at 280 nm assuming an absorbance of 1 equals 1 mg/mL.

Blood collection and processing

All procedures involving collection of human blood from healthy volunteers were in accordance with the Human Research Ethics Committee of the University of Sydney (HREC 2014/244), Alfred Hospital Ethics (Project No: 388/13) and the Helsinki Declaration of 1983. Informed consent was obtained from healthy donors as well as patients with ECMO support. Blood was collected by venesection using a 21G butterfly Terumo needle from 13 healthy donors on no medications (7 male, 6 female, 18-57 years old). The first 5 mL of blood was discarded to avoid any thrombin that may have been generated around the needle insertion site and then drawn into tubes containing 3.2% v/v sodium citrate. Blood from 10 patients with heart failure at a single center, 5 of which had ECMO support, was drawn into citrate/EDTA. Patients with ECMO support received anticoagulation and/or antiplatelet medications based on clinicians' discretion or institutional guideline where patients typically commenced on warfarin, target international normalized ratio 2 to 3, with bridging heparin infusion and aspirin therapy, as well as dipyridamole for those who are considered high risk for thrombosis. Plasma was prepared by twice centrifugation at 800 *g* for 20 minutes at room temperature. On some occasions, healthy donor plasma was incubated with 2.5 μg/mL human recombinant full-length FVIII (Advate, Takeda) for 30 minutes at room temperature. On others, healthy donor plasma was sheared at rates of 2000 or 10 000 s^{-1} for 5 minutes at room temperature using a Kinexus pro+ rheometer.

Biomembrane force probe (BFP) assays

The assembly and experimental procedures of BFP were previously described in detail.[12-14] In brief, a biotinylated human red blood cell (RBC) was aspirated by a micropipette. Then a glass bead was glued to its apex to form a piconewton force sensor (spring constant, 0.3 pN/nm), termed "probe." On the probe bead, both maleimized streptavidin and purified human plasma VWF were covalently linked using an established protocol.[15] On an apposing micropipette, another bead was aspirated and coupled with human recombinant full-length FVIII, termed "target." In certain experiments, the anti-FVIII monoclonal antibody, NB11B2[15], was pre-incubated with SCM–PEG3500–MAL (JenKem) and then incubated with γ-methacryloxypropyltrimethoxy silane beads in phosphate buffer (pH 6.8) overnight at room temperature.[16] To capture FVIII, NB11B2 beads were incubated with FVIII for a further 2 hours before experiment.[12]

In each BFP test cycle, the target micropipette was driven by a linear piezo actuator to touch the probe at subnanometer precision, enabling FVIII-VWF bond formation. Forces during interaction are detected by the deflection of RBC–bead edge as previously described.[17] During the contact phase, the target bead impinged the probe bead with a 20 pN compressive force and 0.2 seconds

contact time to form a bond. In the adhesion frequency assay, "bond" and "no bond" events were enumerated to calculate an adhesion frequency (*P*a) in 200 repeated cycles for each probe–target pair. The single-bond formation of BFP measurements was ensured by tuning VWF and FVIII densities to achieve low adhesion frequencies (≤20%). According to Poisson Statistics,[18] the probe bead was pulled by a single VWF-FVIII bond in most (≥89%) cases. In the force-clamp assay, the target was held at the desired forces (clamp forces) if a "bond" event was detected. Bond lifetimes were measured from when the force reached the clamp force level to when the bond dissociated. Calculation of molecular spring constant, k_{mol}, is presented in supplemental Figure 1.

Quantification of the redox states of VWF disulfide bonds

Dynabeads (2 mg, Life Technologies) were coated with 16 μg of polyclonal anti-VWF (Dako) or anti-FVIII (Affinity Biologicals) antibodies in 1 mL of phosphate-buffered saline on a rotating wheel for 1 hour at 22°C and the excess antibody removed by washing 3 times with 1 mL of phosphate-buffered saline. Plasma (0.7 mL) was incubated with 2 mg of either of the coated beads on a rotating wheel for 1 hour at 22°C. The beads were collected using a magnet, excess plasma aspirated to reduce the volume, and incubated in 0.3 mL of 5 mM ^{12}C-IPA in phosphate-buffered saline containing 10% DMSO for 1 hour at 22°C in the dark to alkylate unpaired Cys thiols in the proteins. The supernatants were aspirated, and the beads incubated with NuPAGE LDS sample buffer (Life Technologies) containing a further 5 mM ^{12}C-IPA for 30 minutes at 60°C. This second labeling step in the presence of sodium dodecyl sulfate facilitates access to buried thiols to ensure that their alkylation is complete.[19] The supernatants were resolved on SDS-PAGE.

The SDS-PAGE gels were stained with colloidal coomassie (Sigma) and the VWF bands excised, destained, dried, incubated with 40 mM dithiothreitol in 25 mM NH_4CO_2 buffer for 30 min at 56°C and washed.[20] The gel slices were incubated with 5 mM ^{13}C-IPA (Cambridge Isotopes) for 1 hour at 22°C in the dark to alkylate the disulfide bond Cys, washed and dried before digestion of proteins with 12.5 ng/μl of trypsin (Promega) in 25 mM NH_4CO_2 and 10 mM $CaCl_2$ overnight at 25°C. Peptides were eluted from the slices with 5% formic acid, 50% acetonitrile. Liquid chromatography, mass spectrometry, and data analysis were performed as described.[21] Cys labeled with ^{12}C-IPA or ^{13}C-IPA has a mass of 133.05276 or 139.07289, respectively. Cys-containing VWF (supplemental Tables 1 and 2) peptides were analyzed. The different redox forms of the Cys residues were quantified from the relative ion abundance (area under the curve, AUC) of peptides labeled with ^{12}C-IPA and/or ^{13}C-IPA. Fraction of the bond unformed is calculated using the relationship: ^{12}C-IPA AUC/(^{12}C-IPA AUC + ^{13}C-IPA AUC). The data was searched for peptides containing free Cys thiols and these were not detected, which indicates that alkylation of unpaired Cys residues by ^{12}C-IPA or ^{13}C-IPA was complete in the proteins.

VWF disulfide-linked peptide analysis

Healthy donor plasmas (0.7 mL) were incubated with polyclonal anti-VWF antibody-coated Dynabeads on a rotating wheel for 1 hour at 22°C. The beads were collected, excess plasma aspirated, and 0.3 mL of 5 mM ^{12}C-IPA in phosphate-buffered saline containing 10% DMSO was added and incubated for 1 hour at 22°C in the dark. The supernatant was aspirated, beads incubated with NuPAGE LDS sample buffer for 30 minutes at 60°C and the supernatants resolved on SDS-PAGE. Gel slices containing the VWF were washed and dried before digestion with 12 ng/μL of chymotrypsin (Roche) overnight at 25°C followed by trypsin (Promega) for 4 hours at 37°C. Reactions were stopped by adding 5% (v/v) formic acid and peptides eluted from the gel slices with 5% formic acid and 50% (v/v) acetonitrile. Peptides in 0.1% formic acid (final volume 12 μL) were resolved on a 35 cm × 75 μm C18 reverse phase analytical column using a 2% to 35% acetonitrile gradient over 22 minutes at a flow rate of 300 nL/min (Thermo Fisher Scientific Ultimate 3000 HPLC), ionized by electrospray ionization at +2.0 kV and analyzed on a Q-Exactive Plus mass spectrometer (Thermo Fisher Scientific) using higher energy collisional induced dissociation fragmentation. Disulfide-linked peptides were searched against human VWF sequence using Byonic analysis software (Protein Metrics). Precursor mass tolerance and fragment tolerance were set at 10 ppm and 0.6 Da, respectively. Variable modifications were defined as oxidized Met, oxidized Cys (mono, di and tri) and glutathionylated Cys with full trypsin cleavage of up to 3 missed cleavages. The false discovery rate was set at 0.01.

Statistical analyses

Data were analyzed in GraphPad Prism 8.2.0 software using unpaired, two-tailed Student *t* test. Differences with a value of $P < .05$ were considered statistically significant and are noted on graphs with *$P < 0.05$, **$P < .01$, ***$P < .001$ and ****$P < .0001$.

Results

Force dependence of binding of FVIII to VWF

VWF and FVIII experience hemodynamic shear forces in the circulation.[12,22-24] To investigate force effects on the VWF-FVIII bond, we employed a BFP and set up the force-clamped dynamic force spectroscopy (DFS) assays to characterize different protein states as previously described.[20,25] Specifically, the BFP was functionalized with VWF on the probe bead (Figure 1A; left) and human recombinant full-length FVIII on the target bead (Figure 1A; right). Two methods of immobilization of FVIII were tested. The FVIII was either covalently attached to the target bead via a PEG3500 linker or captured by a monoclonal antibody, NB11B2, immobilized on the target bead. The NB11B2 antibody binds to the A2 domain of FVIII, which is on the opposite face that binds VWF[26] so will not affect interaction with FVIII.

Upon retraction of the target bead, a "bond" (Figure 1B, blue) or "no bond" (Figure 1B, black) event was signified by the presence of the tensile force in the DFS traces (force vs time). The binding specificity was ensured since the nonspecific binding was $P_a < 0.02$ (Figure 1C), and the rupture force of VWF-FVIII interaction (23.22 ± 0.79 pN) is significantly lower than the force required to break the bond between FVIII and NB11B2 (54.86 ± 2.20 pN) (Figure 1D). The adhesion frequency of VWF-FVIII interaction was in the range 0.1 to 0.2 (Figure 1C), which indicates that >89% of bonds during touch cycles are single-molecular events.[18] Based on this, we then measured VWF-FVIII bond lifetimes at multiple clamped forces from 0 to 60 pN. Intriguingly, the VWF-FVIII interaction displayed a catch-bond behavior in which force first decelerates then accelerates bond dissociation (Figure 1E). Similar

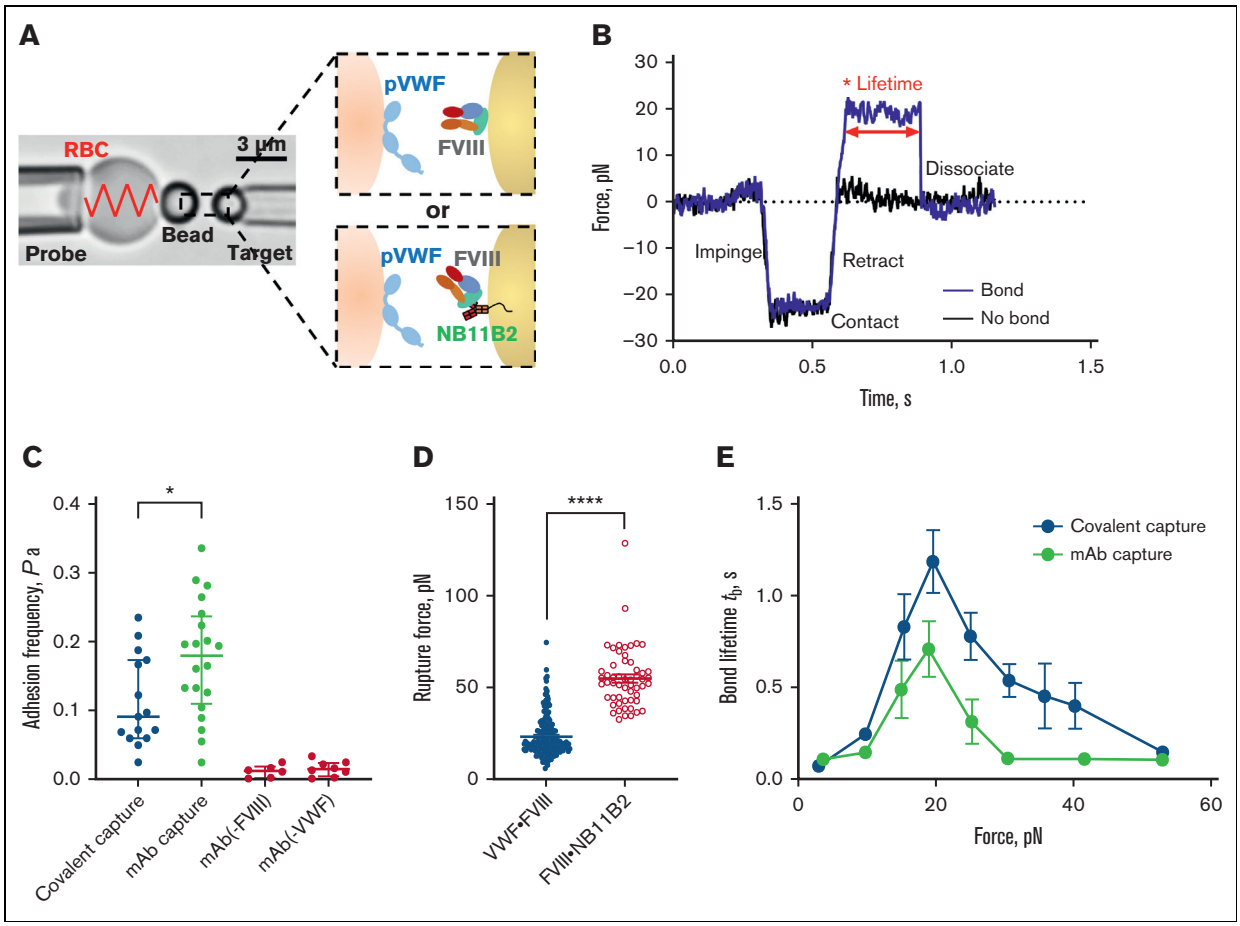

Figure 1. Force dependence of binding of FVIII to VWF. (A) BFP brightfield scheme (left panel) and protein functionalization (right panel). A micropipette-aspirated RBC with a bead attached to the apex (probe, left) was aligned against a bead held by an apposing micropipette (target, right). The probe bead was covalently linked with purified human plasma VWF and streptavidin for attachment of the bead to biotinylated RBC (left). VWF is the focus for interaction with human recombinant full-length FVIII on the target bead (right). The FVIII was either covalently immobilized via a PEG3500 linker or by using NB11B2 antibody that binds to the A2 domain of FVIII on the opposite face that binds VWF. (B) Force vs time traces of 2 representative BFP touch cycles. The target was driven to impinge, contact, and retract the probe. In a "no bond" event, the cycle ended after retraction (black). In a "bond" event (blue), the target was held (marked by *) at clamp force (20 pN) until the bond between probe and target dissociated, signified by the force dropping back to 0, and the lifetime of the bond was measured. (C) Adhesion frequencies of binding of VWF to FVIII immobilized either covalently or using NB11B2 antibody. The negative controls were performed in the absence of either FVIII or VWF. The data points are from 20 touch cycles. Each probe–target pair was tested repeatedly for 200 approach-contact-retract cycles to estimate an adhesion frequency. Errors are mean ± SEM. *$P < .05$ assessed by unpaired, two-tailed Student t test. (D) Rupture force of the VWF-FVIII vs FVIII-NB11B2 bonds. The force applied to the bonds increased until dissociation was detected. The magnitudes of rupture forces were measured at the instant force traces dropped. N ≥ 3 probe–target pairs were tested to obtain mean ± SEM. ****$P < .001$ assessed by unpaired, two-tailed Student t test. (E) Lifetime of VWF-FVIII bonds as a function of clamp force in BFP. The FVIII was immobilized either covalently or using NB11B2 antibody. Results represent mean ± SEM of >50 measurements per point. SEM, standard error of the mean.

catch-bond behaviors were observed regardless of whether FVIII was covalently immobilized on the target bead or captured by the NB11B2 antibody, indicating that the catch-bond behavior is not an artifact of FVIII orientation on the bead.

The structural features of VWF that underpin the force-dependent binding of FVIII were explored by considering type 2N VWD mutations that impair the protection of FVIII in the circulation. The most common mutations at the FVIII binding site in VWF involve disulfide bond cysteine residues. These observations suggest that VWF disulfide bonds are critical motifs for the protective binding of FVIII. Hereby, we examined their redox states in the native plasma protein.

The VWF TIL'-TIL3 domains exists in multiple disulfide-bonded states in the circulation

The redox state of cysteine thiols in the TIL' through E3 domains of VWF was determined using differential cysteine alkylation with a pair of isotopic alkylators and mass spectrometry.[27] Briefly, blood from healthy donors was drawn into citrate as anticoagulant, plasma prepared by centrifugation and VWF collected on antibody-coated magnetic beads (supplemental Figure 2A). The unpaired cysteine thiols in bead-bound VWF were alkylated with a carbon-12 version of 2-iodo-N-phenylacetamide (^{12}C-IPA), the protein isolated by SDS-PAGE (supplemental Figure 2B), the disulfide bonds reduced with dithiothreitol, and the disulfide-bonded

cysteine thiols alkylated with a carbon-13 isotope of IPA (^{13}C-IPA).[20] The ^{12}C-IPA alkylation of VWF was performed in plasma to freeze the redox states before removal of the protein from its ex vivo environment. The VWF was digested with trypsin and peptides quantified by HPLC and identity established by mass spectrometry (supplemental Figure 3). The levels of the different redox forms of the cysteines were determined from the relative abundance of peptides labeled with ^{12}C-IPA and/or ^{13}C-IPA (supplemental Tables 1 and 2). The results are expressed as fraction of the TIL'-TIL3 disulfide that is unformed in the population of VWF monomeric units in the sample. We have used the term "unformed" disulfide bond, as opposed to "reduced" disulfide bond, as reduced implies that the bond was formed at some point and later reduced, for which there is no evidence.

We were able to quantify the redox state of all 5 disulfide bonds (C767-C808, C776-C804, C788-C799, C792-C827 and C810-C821) in the TIL' domain and 1 (C829-C851) of 3 disulfides in the E' domain (Figure 2A-B). The D3, C8-3, TIL3, and E3 domains contain 4, 5, 5, and 3 disulfide bonds, respectively. Of these bonds, we were able to measure the redox state of 2 disulfides in D3 (C889-C1031 and C914-C921), 4 in C8-3 (C1046-C1089, C1060-C1084, C1071-C1111 and C1101-C1126) and 1 in TIL3 (C1130-C1173). These 13 disulfide bonds have been structurally defined in solution[7] (Protein Data Bank [PDB] identifier 2mhq) and/or crystal[11] (PDB identifier 6n29) structures of the VWF domains (Figure 2A-B). All 13 disulfide bonds exist in formed or unformed states in the VWF populations of 13 healthy human donors (7 male, 6 female, 18-57 years old) (Figure 2C). The mean redox state of the 13 disulfides in the 13 healthy donors ranged from 4% to 21% unformed. Individual bonds ranged from 2% to 34% unformed and there was considerable donor-to-donor variation with coefficients of variation ranging from a low of 33.4% for the C776-C804 disulfide to a high of 63.6% for the C1101-C1126 bond, with an average of 49.6%. Analysis of a single plasma sample on 3 separate occasions resulted in an average coefficient of variation of 26.4% for the 13 disulfides (supplemental Figure 4), supporting the donor-to-donor variation. There was no significant gender difference (supplemental Table 3) and no significant age dependence (supplemental Figure 5) in the data cohort, although there is a trend toward more oxidized VWF disulfide bonds in older donors.

The disulfide pairing in the TIL' and E' domains of VWF from NMR and x-ray crystallography structures[7,11] is concordant. We investigated alternative disulfide pairing in these domains from mass spectrometry analysis of disulfide-linked peptides. VWF was immunoprecipitated from healthy 25 and 32 years-old male and female donor plasmas, respectively, digested with trypsin and chymotrypsin, and peptides resolved by HPLC and analyzed by mass spectrometry. A single unpredicted disulfide bond was found linking C827 in the TIL' domain and C829 in the E' domain (supplemental Figure 6) in both samples. This result indicates that C792, C827, C829 and C851 can bond in 3 different configurations: C792-C827, C827-C829, and C829-C851. We have assumed that the C792-C827 and C829-C851 bonds predominate for this analysis.

The extent of unformed bonds in the VWF TIL' to E' domains was compared to the state of 17 disulfide bonds in the 6 C-domains of healthy human donor plasma VWF (5 male, 5 female). The disulfide pairing of the C-domain cysteines is based on structure of the C4 domain[28] and homology with the other domains.[6] The C-domain disulfides are substantially more formed than the bonds in the TIL' to E' domains. The mean redox state of the 17 disulfides in the 10 healthy donors ranged from 0% to 5% unformed, compared to 4% to 21% unformed for the TIL'-E' domain bonds.

An important question is whether VWF arrives in blood as multiple disulfide-bonded states, or a single state is secreted and then converted to multiple forms in the circulation.

Disulfide status of the TIL'-TIL3 domains of recombinant VWF secreted by mammalian cells is indistinguishable from plasma VWF

Full-length recombinant human VWF was expressed in mammalian HEK cells and the VWF in conditioned medium analyzed as for the plasma protein. The redox states of the TIL'-TIL3 domain disulfides of recombinant VWF are indistinguishable from plasma protein (Figure 3). This finding indicates that VWF is constitutively produced and secreted as defined disulfide-bonded states and is not a consequence of postsecretion changes in the blood.

We previously reported that disulfide bonds form in fibrin when fibrin molecules self-associate.[27] We investigated whether disulfides in VWF similarly form when the protein interacts with FVIII.

FVIII binding to VWF results in formation of VWF TIL'-TIL3 disulfides

Three healthy donor plasmas (2 male, 1 female; 25, 25 and 48 years old) that have similar VWF redox states were selected for analysis. Human recombinant full-length FVIII was added to the plasmas at a FVIII:VWF monomer molar ratio of ~1:4 and incubated for 30 minutes. The FVIII was then immunoprecipitated and the VWF bound to FVIII analyzed for redox state of the TIL'-TIL3 disulfides (Figure 4A). The remaining VWF in the depleted plasmas was immunoprecipitated and the redox state of the TIL'-TIL3 disulfides determined. The plasma FVIII to VWF subunit ratio is ~1:50,[29] so endogenous FVIII will not influence the redox state measurements of the VWF disulfides in our studies. As anticipated based on this protein ratio, we could not detect endogenous FVIII peptides in our analysis of plasma VWF.

The mean redox states of 11 of the 12 VWF TIL'-TIL3 disulfides were more oxidized when bound to FVIII ($P < .05$) (supplemental Table 4). The same result was observed when a pegylated recombinant FVIII was used (supplemental Figure 7). Two possibilities could account for this change. A subset of VWF states containing more oxidized disulfide bonds preferentially binds FVIII, or disulfide bonds form in VWF upon FVIII binding. The first possibility implies there would be enrichment of unformed VWF states in plasma as oxidized VWF forms bind FVIII. However, there was no change in the disulfide-bonded states of the VWF remaining in plasma after removal of FVIII:VWF complexes (Figure 4A). This result supports the conclusion that FVIII binding to VWF triggers formation of disulfide bonds in the VWF TIL'-TIL3 domains (Figure 4B).

The consequence of this disulfide formation for the nature of the VWF-FVIII interaction was explored using DFS.

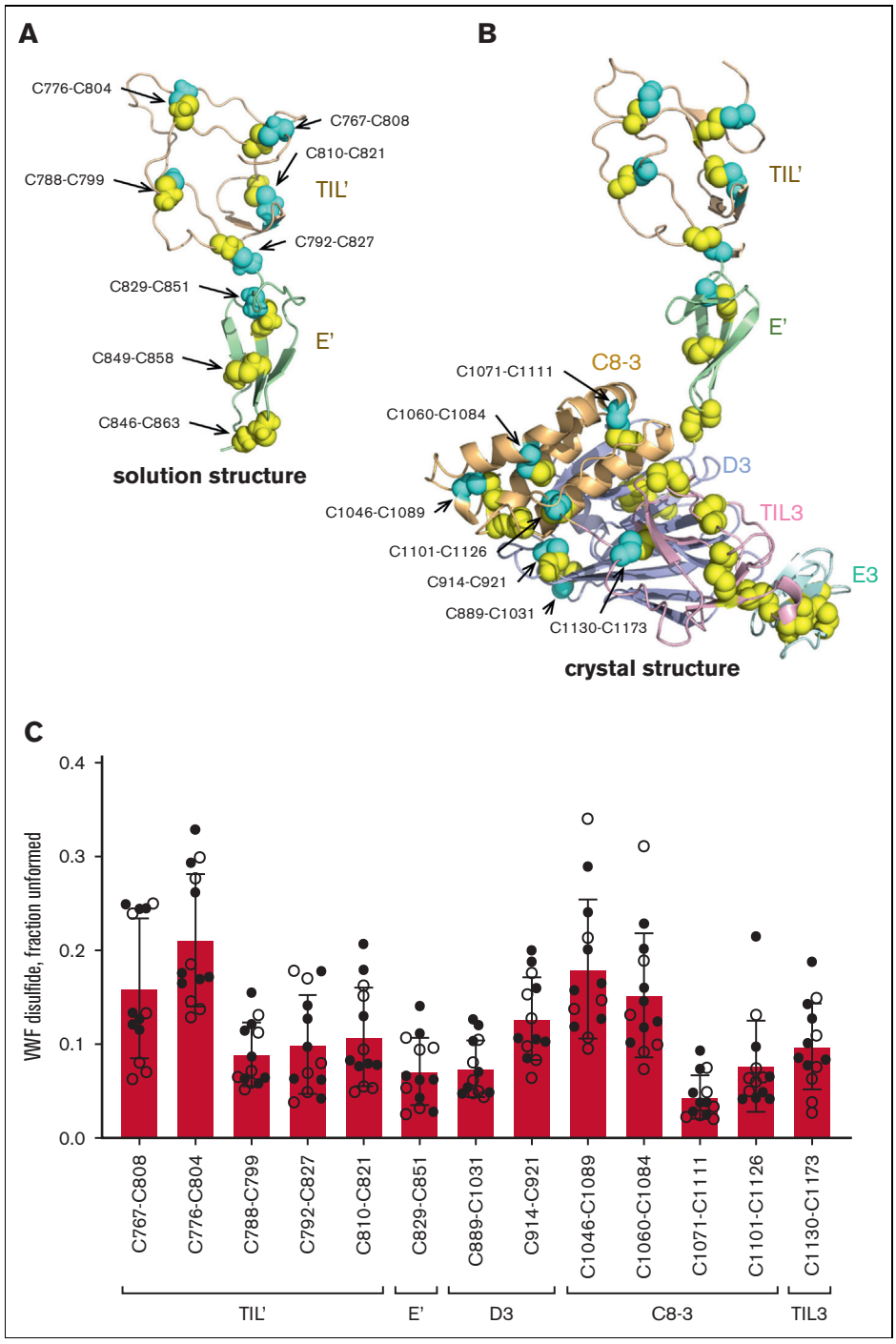

Figure 2. The VWF binding site for FVIII exists in multiple disulfide-bonded states in the circulation. (A) Ribbon representation of the solution structure of the TIL' (residues 764-827 in wheat) and E' (residues 828-863 in light green) domains of VWF[7] (PDB identifier 2mhq). The cysteine residues comprising the eight disulfide bonds are shown as yellow and cyan spheres and the residue numbers indicated. The cysteines in cyan are those residues where the redox state was measured by differential alkylation and by mass spectrometry. (B) Ribbon representation of the crystal structure of the TIL' (residues 764-827 in wheat), E' (residues 828-863 in light green), D3 (residues 864-1037 in light blue), C8-3 (residues 1038-1127 in light orange), TIL3 (residues 1128-1196 in pink) and E3 (residues 1197-1252 in cyan) domains of VWF[11] (PDB identifier 6n29). The cysteine residues comprising the 25 disulfide bonds are shown as yellow and cyan spheres and the residue numbers indicated. The cysteines in cyan are those residues where the redox state was measured by differential alkylation and by mass spectrometry. (C) Redox states of five TIL', 1 E', two D3, four C8-3 and 1 TIL3 disulfides in 13 healthy human donors (7 male - closed symbols; 6 female - open symbols). The bars and errors are mean ± SD. SD, standard deviation.

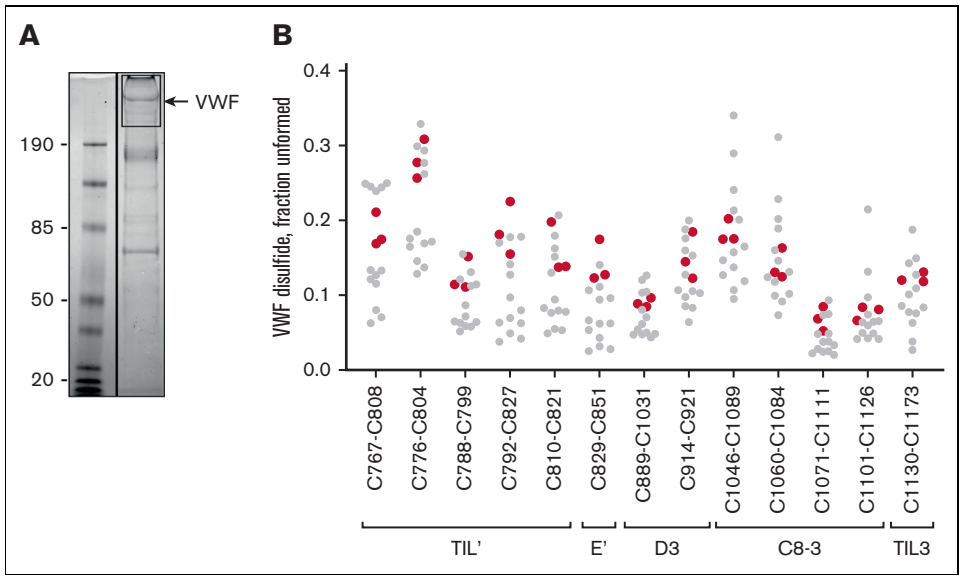

Figure 3. Disulfide status of the TIL'-TIL3 domains of recombinant VWF secreted by mammalian cells is indistinguishable from plasma VWF. (A) Example of ^{12}C-IPA-labeled recombinant human VWF resolved on SDS-PAGE. Molecular mass standards are shown in the left-hand lane. (B) Redox states of the 13 TIL'-TIL3 domain disulfide bonds in 3 different preparations of recombinant VWF (red symbols). The redox states of the 13 healthy donor VWF disulfides (Figure 2C) are shown for reference (gray symbols).

Blocking disulfide formation in VWF prevents stiffening of the VWF-FVIII bond in response to force

To prevent disulfide formation in purified plasma VWF, the unpaired cysteine thiols were alkylated with ^{12}C-IPA and the unreacted ^{12}C-IPA removed by filtration. The effect of blocking disulfide formation in VWF on the force dependence of the interaction was measured using the BFP (Figure 1).

The VWF-FVIII adhesion frequencies in the absence or presence of IPA alkylation were comparable. This effective 2-dimensional avidity measurement on BFP confirms that IPA alkylation of VWF did not inhibit the binding of FVIII (Figure 5A). As for untreated VWF, the adhesion frequency was in the range 0.1 to 0.2 which indicates that >89% of bonds during touch cycles are single-molecular events.[18] We then measured VWF-IPA·FVIII bond lifetimes at clamped forces of 0 to 60 pN. Notably, IPA-treated VWF dissociated much slower from FVIII at the low force regime (Figure 5B, lifetime of 1.02 ± 0.18 seconds) than untreated VWF (0.11 ± 0.02 seconds), while the bond lifetime quickly shortened when the force increased as a slip bond. These results demonstrate that the fundamental nature of the interaction of VWF with FVIII is dependent on dynamic disulfide formation in VWF.

To better understand the requirement for VWF disulfide bond formation for productive binding of FVIII, we measured the molecular spring constant (k_{mol}) as a function of clamped force[14] (supplemental Figure 1). Interestingly, the molecular spring constant between untreated VWF and FVIII stiffened when the clamp force increased from 10 pN (0.1922 ± 0.0186 pN/nm) to 30 pN (0.3794 ± 0.0128 pN/nm), while the k_{mol} at 20 pN clamp force behaves as a mixed distribution of both low and high spring constant (Figure 5C). In sharp contrast, there was no significant spring stiffening for the VWF-IPA·FVIII interaction in the same force range (10 pN: 0.1222 ± 0.0087 pN/nm; 20 pN: 0.1341 ± 0.0081 pN/nm; 30 pN: 0.1481 ± 0.0055 pN/nm) (Figure 5C). This difference may explain the catch-bond behavior of the native interaction since a higher magnitude of force is required to separate the proteins. However, when disulfide bonds in VWF are prevented from forming, the fixed molecular spring constant is not able to stabilize the interaction at increasing force resulting in a slip-only bond phenotype.

Considering the requirement for disulfide bond formation in VWF for FVIII binding under force, an important consideration is whether the VWF TIL'-TIL3 disulfides are static or dynamic, that is can they change state in the circulation. VWF is subject to hemodynamic forces that reversibly transforms its structure from a loosely coiled ball to an elongated form and controls its adhesiveness.[30-32] We therefore examined clinically relevant mechanical effects on the disulfide states of the TIL'-TIL3 domains.

The redox state of VWF TIL'-TIL3 disulfides are changed by mechanical shearing in vitro and in patients with heart failure subjected to extracorporeal membrane oxygenation (ECMO)

Healthy donor plasma was subjected to physiological (2000 s^{-1}) and pathophysiological (10 000 s^{-1}) fluid shear forces.[33-35] The 2000 s^{-1} shear rate did not change the redox state of the VWF TIL'-TIL3 disulfides, while the pathological fluid shear caused reduction of all 13 disulfides (Figure 6A). The high fluid shear, therefore, triggered global cleavage of VWF disulfides, indicating that the bonds are dynamic in plasma. A clinical situation associated with high blood shear is the use of ECMO support to treat patients with refractory heart failure. The ECMO device subjects blood to high shear and influences hemostasis and thrombosis in the patients.[36]

Six of the 13 VWF TIL'-TIL3 disulfides were significantly ($P < .001$) more reduced in patients with heart failure receiving ECMO than in patients not receiving this mechanical assist (Figure 6B). The VWF

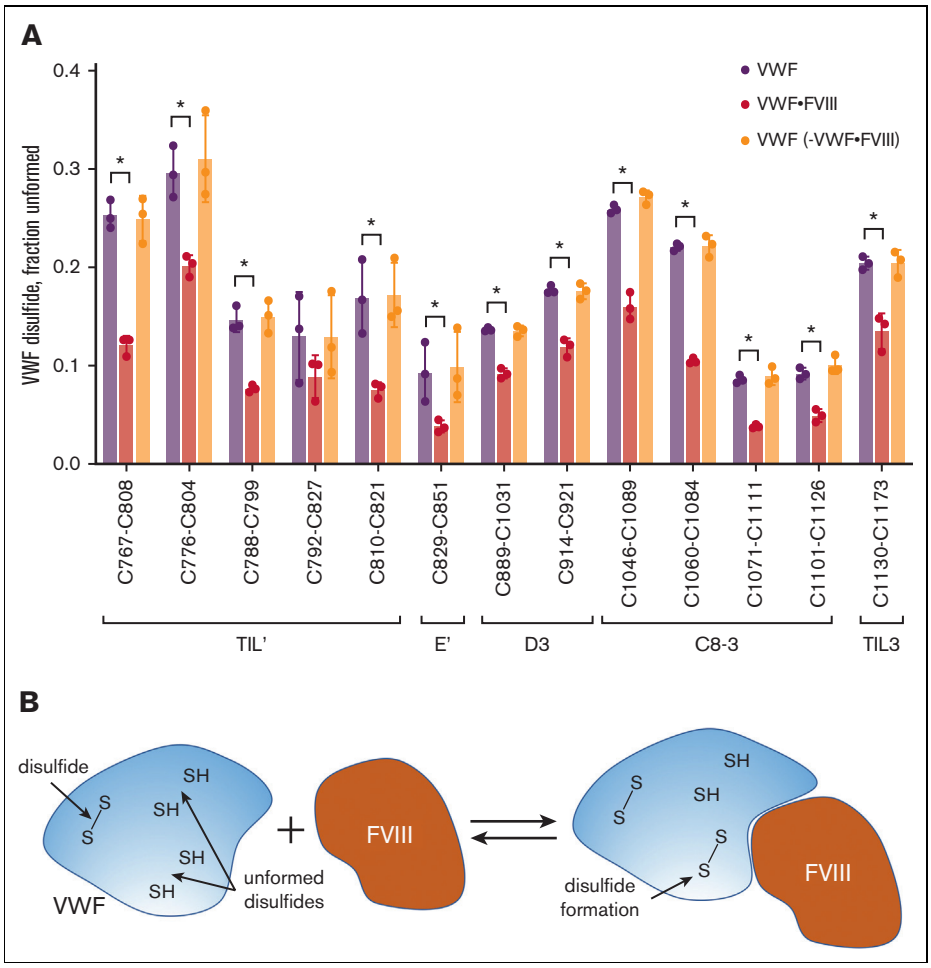

Figure 4. FVIII binding to VWF results in formation of VWF TIL'-TIL3 disulfides. (A) Comparison of the redox states of the VWF TIL'-TIL3 disulfides in 3 healthy human donors (2 males, 1 female) (purple symbols), the plasma VWF bound to human recombinant full-length FVIII (red symbols) and the unbound VWF in plasma following removal of VWF-FVIII complexes (orange symbols). The bars and errors are mean ± SD. Parametric unpaired *t* test was used to evaluate differences between groups. Significant difference ($P < .05$) between VWF and VWF-FVIII groups is indicated by *. There was no significant difference between the VWF and VWF – VWF-FVIII groups. (B) Model for disulfide-dependent interaction of VWF with FVIII. We suggest that the different disulfide-bonded forms of the TIL'-TIL3 domains of VWF and the inherent conformational flexibility therein facilitate initial interactions with FVIII, and subsequent disulfide formation in VWF results in a productive interaction.

and FVIII characteristics of the patients are reported in supplemental Table 5. A notable feature is the loss of ultra-large VWF multimers in the patients receiving ECMO that is in accordance with previous reports.[36] Considering that the disease severity and therapeutic interventions in these patients is highly variable, the result implies that reduction of the VWF disulfides is a result of the ECMO-related blood shear. Importantly, this finding indicates that the covalent forms of VWF can change in this extreme hemodynamic environment, which has significant implications for its role in hemostatic disorders.

Discussion

In addition to prolonging the half-life of FVIII in the circulation, VWF also delivers FVIII to the developing thrombus. At the thrombus, the FVIII dissociates from VWF and incorporates into the tenase complex where it catalyzes factor Xa and thrombin formation. The catch-bond behavior of the VWF-FVIII interaction suggests a mechanism for this transfer. The bell-shaped force dependence indicates that FVIII will dissociate from VWF at low and high shear forces. Previous studies on platelets[22-24] and its glycoprotein Ibα receptor[12,23] have demonstrated that the single-molecule binding forces tested in our BFP assays are well-correlated with the forces platelets experience during in vivo thrombosis, and by extension VWF. VWF-FVIII incorporated into a developing thrombus will experience different shear forces than when circulating. This change in forces could be a trigger for FVIII dissociation from VWF and transfer to tenase.

Cysteine mutations at the FVIII binding site in VWF result in defective FVIII binding and consequently low levels of circulating FVIII. Eighteen VWD cysteine mutants involving 14 disulfide bonds in the VWF TIL'-TIL3 domains have been reported (supplemental Figure 8A). Of these mutations, 5 (C788R/Y, C804F, C858F/S C1060R/Y and C1225G) result in impaired binding of FVIII but not production of VWF, or type 2N VWD. Three of these 5 disulfide bonds were measured in this study and found to exist in formed and unformed states in plasma VWF: C788-C799, C776-C804, C1060-C1084. Considering that these bonds naturally exist in unformed states, it is not unexpected that lack of the associated disulfide bond has no impact on VWF maturation and secretion of

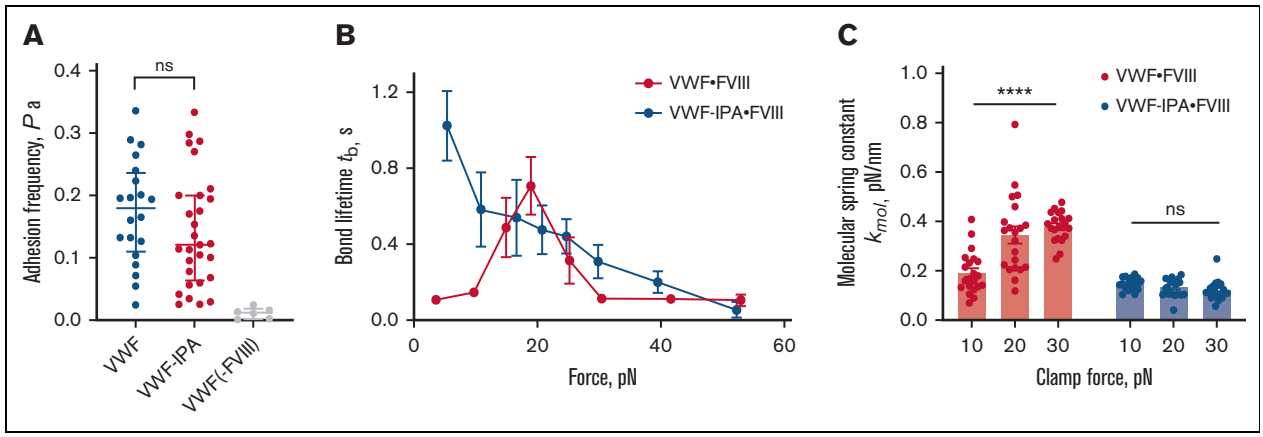

Figure 5. Blocking disulfide formation in VWF prevents stiffening of the VWF-FVIII bond in response to force. VWF or VWF-IPA on the bead was the focus for interaction with human recombinant full-length FVIII on the target. The FVIII was immobilized using NB11B2 antibody that binds to the A2 domain of FVIII on the opposite face that binds VWF. (A) Adhesion frequencies of binding of VWF or VWF-IPA to FVIII. The negative control is performed in the absence of FVIII. The data points are from 20 or 29 touch cycles for VWF or VWF-IPA, respectively. Each probe–target pair was tested repeatedly for 200 approach-contact-retract cycles to estimate an adhesion frequency. Errors are mean ± SEM. (B) Lifetime of VWF-FVIII or VWF-IPA·FVIII bonds as a function of clamp force in BFP. Results represent mean ± SEM of >50 measurements per point. (C) The molecular spring constant (k_{mol}) of the VWF-FVIII and VWF-IPA·FVIII bonds during the retraction phase of the BFP cycle at 10, 20, and 30 pN clamp force levels. Data at each force level were obtained from >20 points. Errors are mean ± SEM. ****$P < .0001$, assessed by an unpaired, two-tailed Student t test.

some type 2N mutants. Our observations imply that impaired FVIII binding of the mutants may not be due to disruption of disulfide bonds and concomitant structural changes in the polypeptide, but rather replacement of the cysteines with nonisosteric residues introduce steric factors that impede FVIII binding. Some of the VWD disulfide bond cysteines in the TIL'-TIL3 domains are exposed on the surface of the domain while others are buried in the structure (supplemental Figure 8B), so steric changes could involve mutated cysteines that directly contact FVIII while the buried cysteine mutants may perturb the underlying structure of the domain. It is a strong possibility that mutation of the cysteines impairs formation of the disulfides triggered by FVIII binding that are required for a productive catch-bond.

The disulfides in the TIL' through E3 domains of VWF naturally exist in unformed states in significant fractions of healthy donor plasma VWF. Some TIL'-TIL3 disulfides are unformed in as little as 1 in 50 monomeric VWF units in some individuals (C1071-C1111), while others are unformed in as many as 1 in 3 VWF monomeric units (C776-C804, C1046-C1089, and C1060-C1084 bonds). The redox state of the TIL'-TIL3 disulfides in human plasma VWF was indistinguishable from human recombinant VWF produced in HEK cells. This result indicates that the different disulfide-bonded forms of VWF are constitutively produced by cells, that is the redox states of the VWF TIL'-TIL3 disulfides are set in place during folding and maturation of the protein. We have described the same phenomenon in human fibrinogen and α2-macrogobulin.[27] In contrast to these 2 plasma proteins, there is wide variation in individual healthy donor TIL'-TIL3 disulfide redox states. The coefficients of variation for the unformed states of 13 fibrinogen disulfide bonds, for example, ranged from 3.9% to 16.5% in 10 healthy donors,[27] which is remarkably small donor-to-donor variation. The pattern of the redox state of the 13 VWF disulfides in individuals tends to be consistent, however, with all bonds either more or less formed in individual healthy donors (supplemental Figure 4).

Binding of FVIII to VWF results in partial formation of 12 of the 13 VWF TIL'-TIL3 disulfide bonds that is required for force-induced stiffening of VWF-FVIII interaction. The same dynamic cysteine/disulfide chemistry was observed in fibrin when the protein polymerizes.[27] The different disulfide-bonded forms of VWF are predicted to have different dynamics and conformational flexibility. We suggest that the inherent conformational malleability of the different covalent forms increases the chances of favorable interactions with FVIII, particularly in the fluid shear forces of the circulation, and the disulfide bond formation triggered by favorable interactions results in a productive catch-bond. Presumably, binding of FVIII changes the structure of VWF in such a way as to enable disulfide bond formation at the FVIII binding site and stiffening of the interaction. Although, we cannot rule out contributions from structural changes in VWF domains distant from TIL'–TIL3 to stiffening of the bond. This aspect of the model is analogous to the "induced fit" model for enzyme-substrate interaction proposed by Koshland.[37] The induced fit model states that binding of a substrate to an enzyme causes a change in the shape of the enzyme so as to enhance its activity. In terms of the current study, binding of FVIII to VWF causes a change in the shape of VWF so as to enable disulfide bond formation required for catch-bond behavior.

Hemodynamic force can not only unfold VWF to expose platelet binding sites in A domains,[31,38,39] but also cause reduction of the VWF TIL'-TIL3 disulfide bonds. Distorting a protein has been demonstrated to enhance disulfide bond cleavage through changes in the alignment of the sulfur atoms involved in the cleavage.[25,40,41] Bond cleavage, though, requires a source of electrons such as provided by small molecule or protein thiols.[42] Future studies will explore the role of small molecule and protein plasma thiols in the VWF disulfide cleavage. It will also be important to determine if the different multimer sizes of VWF exist in different redox states as platelet tethering capacity in flowing blood is a

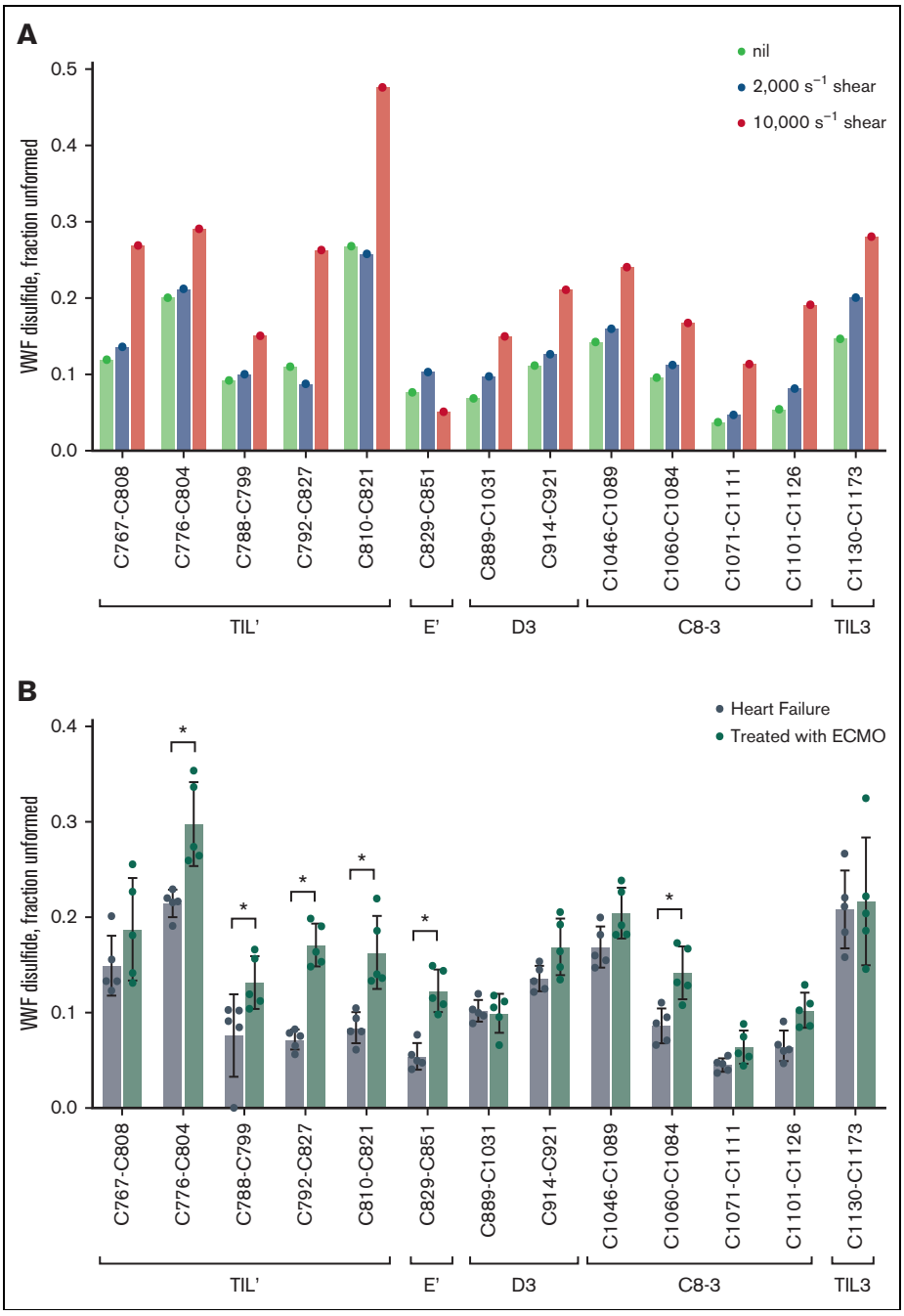

Figure 6. The redox state of VWF TIL'-TIL3 disulfides are changed by mechanical shearing in vitro and in patients with heart failure subjected to ECMO. (A) Redox states of the 13 TIL'-TIL3 VWF disulfides from a single healthy donor plasma (32 year-old male) sheared at rates of 2000 or 10 000 s^{-1} for 5 minutes. Shearing at 10 000 s^{-1} results in reduction of all 13 VWF disulfides. (B) Redox states of the 13 TIL'-TIL3 VWF disulfides in 5 patients with heart failure and 5 patients with heart failure subjected to ECMO. The bars and errors are mean ± SD. Significant differences ($P < .01$) in the redox state of VWF disulfides are indicated by stars. Parametric unpaired *t* test was used to evaluate differences between groups.

function of multimer size. The biggest multimers are also more susceptible to hemodynamic drag forces, which we have shown changes the balance of the redox states.

Acknowledgments

The authors thank Joyce Chiu for assistance with the disulfide-linked peptide analysis, Carmen Coxon for the FVIII antibody NB11B2, Elizabeth Gardiner, Amanda Davis, Deirdre Murphy and Robert Andrews for the heart failure patient plasmas, and Marc Ellis for assistance with shearing of plasma.

This research was funded by the National Health and Medical Research Council of Australia (grants 1110219, 1143400, 1143398, and 2003904), Australian Research Council (200101970), a Senior Researcher grant (P.J.H.), and an Early-Mid Career Research grant (L.A.J.) from the NSW Cardiovascular Research Capacity Program.

L.A.J. is an ARC DECRA fellow (DE190100609) and National Heart Foundation Future Leader fellow (105863).

Authorship

Contribution: P.J.H. conceived the study and designed experiments; D.B., H.J.W., H.-G.W., and Y.C.Z. designed and performed the experiments; L.A.J. supervised the BFP studies; and P.J.H. and L.A.J. wrote the manuscript.

Conflict-of-interest disclosure: The authors declare no competing financial interests.

ORCID profiles: H.J.W., 0000-0002-4575-6501; Y.C.Z., 0000-0002-1802-2318; L.A.J., 0000-0002-7591-0864.

Correspondence: Philip Hogg, The Centenary Institute, Locked Bag No. 6, Newtown, NSW 2042, Australia; email: phil.hogg@sydney.edu.au.

References

1. Perez-Riverol Y, Bai J, Bandla C, et al. The PRIDE database resources in 2022: a hub for mass spectrometry-based proteomics evidences. *Nucleic Acids Res*. 2022;50(D1):D543-D552.
2. Sadler JE. Biochemistry and genetics of von Willebrand factor. *Annu Rev Biochem*. 1998;67:395-424.
3. Vlot AJ, Koppelman SJ, Meijers JC, et al. Kinetics of factor VIII-von Willebrand factor association. *Blood*. 1996;87(5):1809-1816.
4. Goodeve AC. The genetic basis of von Willebrand disease. *Blood Rev*. 2010;24(3):123-134.
5. Foster PA, Fulcher CA, Marti T, Titani K, Zimmerman TS. A major factor VIII binding domain resides within the amino-terminal 272 amino acid residues of von Willebrand factor. *J Biol Chem*. 1987;262(18):8443-8446.
6. Zhou YF, Eng ET, Zhu J, Lu C, Walz T, Springer TA. Sequence and structure relationships within von Willebrand factor. *Blood*. 2012;120(2):449-458.
7. Shiltagh N, Kirkpatrick J, Cabrita LD, et al. Solution structure of the major factor VIII binding region on von Willebrand factor. *Blood*. 2014;123(26):4143-4151.
8. Fuller JR, Knockenhauer KE, Leksa NC, Peters RT, Batchelor JD. Molecular determinants of the factor VIII/von Willebrand factor complex revealed by BIVV001 cryo-electron microscopy. *Blood*. 2021;137(21):2970-2980.
9. Pietu G, Ribba AS, Cherel G, et al. Epitope mapping of inhibitory monoclonal antibodies to human von Willebrand factor by using recombinant cDNA libraries. *Thromb Haemost*. 1994;71(6):788-792.
10. Jorieux S, Gaucher C, Pietu G, Cherel G, Meyer D, Mazurier C. Fine epitope mapping of monoclonal antibodies to the NH2-terminal part of von Willebrand factor (vWF) by using recombinant and synthetic peptides: interest for the localization of the factor VIII binding domain. *Br J Haematol*. 1994;87(1):113-118.
11. Dong X, Leksa NC, Chhabra ES, et al. The von Willebrand factor D'D3 assembly and structural principles for factor VIII binding and concatemer biogenesis. *Blood*. 2019;133(14):1523-1533.
12. Ju L, Dong JF, Cruz MA, Zhu C. The N-terminal flanking region of the A1 domain regulates the force-dependent binding of von Willebrand factor to platelet glycoprotein Ibalpha. *J Biol Chem*. 2013;288(45):32289-32301.
13. Wang H, Zhou F, Guo Y, Ju LA. Micropipette-based biomechanical nanotools on living cells. *Eur Biophys J*. 2022;51(2):119-133.
14. Obeidy P, Wang H, Du M, et al. Molecular spring constant analysis by biomembrane force probe spectroscopy. *J Vis Exp*. 2021;(177).
15. Ju L. Dynamic force spectroscopy analysis on the redox states of protein disulphide bonds. *Methods Mol Biol*. 2019;1967:115-131.
16. Chen Y, Liu B, Ju L, et al. Fluorescence biomembrane force probe: concurrent quantitation of receptor-ligand kinetics and binding-induced intracellular signaling on a single cell. *J Vis Exp*. 2015;(102):e52975.
17. An C, Hu W, Gao J, et al. Ultra-stable biomembrane force probe for accurately determining slow dissociation kinetics of PD-1 blockade antibodies on single living cells. *Nano Lett*. 2020;20(7):5133-5140.
18. Chesla SE, Selvaraj P, Zhu C. Measuring two-dimensional receptor-ligand binding kinetics by micropipette. *Biophys J*. 1998;75(3):1553-1572.
19. Pijning AE, Butera D, Hogg PJ. Not one, but many forms of thrombosis proteins. *J Thromb Haemostasis*. 2022;20(2):285-292.
20. Butera D, Passam F, Ju L, et al. Autoregulation of von Willebrand factor function by a disulfide bond switch. *Sci Adv*. 2018;4(2):eaaq1477.
21. Chiu J. Quantification of the redox state of protein disulphide bonds. *Methods Mol Biol*. 2019;1967:45-63.
22. Chen Y, Ju LA, Zhou F, et al. An integrin αIIbβ3 intermediate affinity state mediates biomechanical platelet aggregation. *Nat Mater*. 2019;18(7):760-769.
23. Yago T, Lou J, Wu T, et al. Platelet glycoprotein Ibalpha forms catch bonds with human WT vWF but not with type 2B von Willebrand disease vWF. *J Clin Invest*. 2008;118(9):3195-3207.
24. Ju L, McFadyen JD, Al-Daher S, et al. Compression force sensing regulates integrin αIIbβ3 adhesive function on diabetic platelets. *Nat Commun*. 2018;9(1):1087.
25. Passam F, Chiu J, Ju L, et al. Mechano-redox control of integrin de-adhesion. *Elife*. 2018;7:e34843.
26. Coxon CH, Yu X, Beavis J, et al. Characterisation and application of recombinant FVIII-neutralising antibodies from haemophilia A inhibitor patients. *Br J Haematol*. 2021;193(5):976-987.
27. Butera D, Hogg PJ. Fibrinogen function achieved through multiple covalent states. *Nat Commun*. 2020;11(1):5468.

28. Xu ER, von Bulow S, Chen PC, et al. Structure and dynamics of the platelet integrin-binding C4 domain of von Willebrand factor. *Blood*. 2019;133(4):366-376.

29. Pipe SW, Montgomery RR, Pratt KP, Lenting PJ, Lillicrap D. Life in the shadow of a dominant partner: the FVIII-VWF association and its clinical implications for hemophilia A. *Blood*. 2016;128(16):2007-2016.

30. Steppich DM, Angerer JI, Sritharan K, et al. Relaxation of ultralarge VWF bundles in a microfluidic-AFM hybrid reactor. *Biochem Biophys Res Commun*. 2008;369(2):507-512.

31. Schneider SW, Nuschele S, Wixforth A, et al. Shear-induced unfolding triggers adhesion of von Willebrand factor fibers. *Proc Natl Acad Sci U S A*. 2007;104(19):7899-7903.

32. Siedlecki CA, Lestini BJ, Kottke-Marchant KK, Eppell SJ, Wilson DL, Marchant RE. Shear-dependent changes in the three-dimensional structure of human von Willebrand factor. *Blood*. 1996;88(8):2939-2950.

33. Bark DL Jr, Ku DN. Wall shear over high degree stenoses pertinent to atherothrombosis. *J Biomech*. 2010;43(15):2970-2977.

34. Li MX, Beech-Brandt JJ, John LR, Hoskins PR, Easson WJ. Numerical analysis of pulsatile blood flow and vessel wall mechanics in different degrees of stenoses. *J Biomech*. 2007;40(16):3715-3724.

35. Banerjee RK, Back LH, Back MR, Cho YI. Physiological flow analysis in significant human coronary artery stenoses. *Biorheology*. 2003;40(4):451-476.

36. Murphy DA, Hockings LE, Andrews RK, et al. Extracorporeal membrane oxygenation-hemostatic complications. *Transfus Med Rev*. 2015;29(2):90-101.

37. Koshland DE. Application of a theory of enzyme specificity to protein synthesis. *Proc Natl Acad Sci U S A*. 1958;44(2):98-104.

38. Barg A, Ossig R, Goerge T, et al. Soluble plasma-derived von Willebrand factor assembles to a haemostatically active filamentous network. *Thromb Haemost*. 2007;97(4):514-526.

39. Fu H, Jiang Y, Yang D, Scheiflinger F, Wong WP, Springer TA. Flow-induced elongation of von Willebrand factor precedes tension-dependent activation. *Nat Commun*. 2017;8(1):324.

40. Wiita AP, Ainavarapu SR, Huang HH, Fernandez JM. Force-dependent chemical kinetics of disulfide bond reduction observed with single-molecule techniques. *Proc Natl Acad Sci U S A*. 2006;103(19):7222-7227.

41. Wiita AP, Perez-Jimenez R, Walther KA, et al. Probing the chemistry of thioredoxin catalysis with force. *Nature*. 2007;450(7166):124-127.

42. Chiu J, Hogg PJ. Allosteric disulfides: sophisticated molecular structures enabling flexible protein regulation. *J Biol Chem*. 2019;294(8):2949-2960.